2004

Allometric Scaling and Instability in Electrospinning

Ji-Huan He, *Donghua University*
Yu-Qin Wan
Jian-Yong Yu

©Freund Publishing House Ltd. International Journal of Nonlinear Sciences and Numerical Simulation 5(3), 243-252, 2004

Allometric Scaling and Instability in Electrospinning*

Ji-Huan He[a,b], Yu-Qin Wan[b,c], Jian-Yong Yu[b,c]**

a. College of Science, Donghua University, 1882 Yan'an Xilu Road, Shanghai 200051, People's Republic of China. Email: jhhe@ dhu.edu.cn

b. Key Lab of Textile Technology, Ministry of Education, Shanghai, China

c. College of Textiles, Donghua University, Shanghai, China

Abstract

The regulation of scale and bifurcation-like instability in electrospinning are intriguing and enduring problems after the technology was invented by Formhals in 1934. Regulatory mechanisms for controlling the radius of electrospun fibers are clearly illustrated in the different states. Generally, the relationship between radius r of jet and the axial distance z from nozzle can be expressed as an allometric equation of the form $r \sim z^b$, the values of the scaling exponent (b) for the initial steady stage, instability stage, and terminal stage are respectively –1/2, –1/4, and 0. Allometry in economy, biology, turbulence, astronomy, neural resistance, conductive textile, and macromolecule viscosity is also briefly illustrated.

Keywords: electrospinning, polymer, nanofiber, allometric scaling, turbulence, intelligent textile, Mark–Houwink relationship, Hodgkin-Huxley model, neural model, resistance, modified Ohm law

Tyger! Tyger! Burning bright
in the forests of the night
What immortal hand or eye
Could frame thy fearful symmetry?
By William Blake(1757-1827)
Songs of Experience

1. Introduction

Electrospinning[1,2,3] has been recognized as an efficient technique for the fabrication of polymer nanofibers, which have several amazing characteristics such as very large surface area to volume ratio (this ratio for a nanofiber can be as large as 100 times of that of a microfiber), flexibility in surface functionalities, and superior mechanical performance (e.g. stiffness and tensile strength) compared with any other known form of the material. These outstanding properties make the polymer nanofibers to be optimal candidates for many important applications. Various polymers have been successfully electrospun into ultrafine fiber in recent years mostly in solvent solution and some in melt form. The electrospun nanofibers can find wide applications in various areas, such as air filtration, water filtration, agricultural nanotechnology, wound dressing, bone tissue engineering, drug delivery, just say few. The procedure involves applying a very high voltage to a capillary and pumping a polymer solution through it. Nanofibers of polymer collect as a nonwoven fabric on a grounded plate below the capillary.

In this paper, we will theoretically study the allometric scaling laws in different stages of electrospinning. The relationship between radius r of jet and the axial distance z from nozzle has been the subject of regular investigation since

* The work is supported by grant 10372021 from National Natural Science Foundation of China
** Contributing author.

the electrospinning process was first patented by Formhals in 1934, and it was considered that the allometry $r \sim z^{-1/4}$ [4~9]is a ubiquitous scaling law in electrospinning, our study challenges this view, and we point out that different stages of electrospinning obeys different scaling laws.

2. Allometric Scaling in Nature

Scaling and dimensional analysis actually started with Newton[10], and allometry exists everywhere in our day life and scientific activity. We begin with the well-known Kepler's 3rd law, which says[11]

The squares of the periods of revolution around the Sun are proportional to the cubes of the distances.

In allometric form, the Kepler's 3rd law can be expressed in the form

$$T \sim R^{3/2}, \tag{2.1}$$

where R is the distance from the planet to the Sun , T is the period.

Iovane[12] suggested a scale invariant law for astrophysical structures:

$$N \sim R^{2/3}, \tag{2.2}$$

where R is the radius of the astrophysical structure, N the number of nucleons into the structures.

Similar phenomenon arises from our daily life observation. The best known example is the simple pendulum, with the period:

$$T \sim R^{1/2}, \tag{2.3}$$

where R is the length of pendulum.

Allometry is widely applied in biology, the most fruitful achievement is the allometric scaling relationship relating metabolic rate (B) to body mass (M)[13~16]

$$B \sim M^{b}, \tag{2.4}$$

where b is the scaling exponent. The value of the scaling exponent is a point of contention through the open literature, within which arguments for and against $b = 3/4$ and $b = 2/3$.

He and Chen[13] tried to explain the biological allometry by taking into account the dimension of the organisms

$$B \sim M^{D/(D+1)}, \tag{2.5}$$

where D is the dimension of the organism construction, for example D=2 for a leaf, and D=3 for heart.

Generally, the form of an allometric relation can be expressed as

$$Y \sim X^{b}, \tag{2.5}$$

where Y and X are two measures describing an organism or an event, such as the weight of the antlers X and total weight of a deer Y. The exponent is critical important, and it is relevant to space dimension, so (2.5) can be re-written in the form

$$Y \sim X^{D/(D+1)}, \tag{2.6}$$

or

$$Y \sim X^{k/(D+1)}, \tag{2.7}$$

where D is dimension of the discussed problem, k is an integral. For example, D=1 for a planet moving around a circle, the exponent should be 1/2 or multiplier of 1/2, see (2.1).

Instead of the number of nucleons, if N in (2.2) is the number of the electrons, which move around a surface of a sphere, i.e. D=2, leading to (2.2).

Allometry was developed independently somewhat later in the biological sciences. Scaling in 19th century biology took the form of allometric relations to interrelate the growth of various parts of an organism. Huxley[17] gave a number of examples of such systems in biology.

In another area, evolutionary biology, a deterministic relation was observed between the central moments of a spatially heterogeneous distribution of the number of species, that is , the variance in the number of species Y is proportional to a power of the mean number of

species *X*, in direct analogy with the allometric relation[18]. Economics is another discipline in which such relations appear. Pareto[19] determined that the probability density *Y* for the distribution of income could be related to the level of income *X*, where the power-law index was typically $b=-3/2$.

Benzi's interesting introduction to turbulence[20] leads the present authors to the following hypothesis: the dependence of a fluid variable *Y* on the Reynolds number Re is typically expressed using the power function

$$Y \sim \mathrm{Re}^{b}, \tag{2.8}$$

where b is the power exponent, the Reynolds number is defined as $\mathrm{Re}=UL/\nu$, where *U* and *L* are the typical velocity and scale of the flow, respectively, and ν is the kinematic viscosity due to molecular forces.

When b=1 the relationship is isometric and when $b\neq 1$ the relationship is allometric. Isometry can be found in laminar flow (e.g. the Poiseuille formula). When Re increases, the flow switches isometry to allometry. We write (2.8) in the form:

$$Y \sim \mathrm{Re}^{D/(D+1)}. \tag{2.9}$$

Now considering a particle's motion in turbulence(see Fig. 1), the velocity varies along the pathline. The motion is an approximate one-dimensional one(D=1), so we predict that

$$\frac{\partial V}{\partial s} \sim \mathrm{Re}^{1/2}, \tag{2.10}$$

where *V* the velocity of the particle.

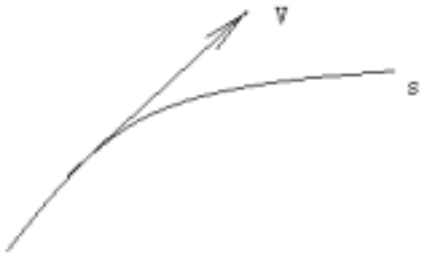

Fig.1 *An approximate one-dimensional flow*

The prediction (2.10) is same as that in [20]. For a fully developed turbulence(see the picture in Benzi's paper[20]), it is of three dimensional construction(D=3), so we have

$$Y \sim \mathrm{Re}^{3/4}, \tag{2.11}$$

or the scaling exponent b in (2.8) characteristically takes a limited number of values, all of which are simple multiples of 1/4. For example, the Kolmogorov length, η, scales as[20,21]

$$\eta \sim \mathrm{Re}^{-3/4}. \tag{2.12}$$

Allometric scaling laws were also found in other systems as well. One example is the drainage basin of a river. In[22] it is shown that the mass of the river and the area of the drainage basin follow a scaling law with an exponent of 2/3. An example of a one-dimensional system that exhibits scaling is given in [23] where the flow through a tube is investigated. It is found that the amount of water in the tube and its length are related by a scaling law with exponent 1/2[23].

Allometry is very effective to quantitative analysis. Now we consider the relation between viscosity of macromolecular solution and molecular weight.

Viscosity is caused by chemical forces acting on macromolecules, among others, the weak electric force of surface charge is dominant. As we know that the surface charge distributes on the outside of the system of macromolecules, so D=2, leading to the result

$$\eta \sim M_w^{2/3}, \tag{2.13}$$

where η is the viscosity, M_w molecular weight.

Tacx *et al*.[24] have obtained the following Mark–Houwink relationship for PVA in water:

$$\eta = 6.51\times 10^{-4} M_w^{0.628}. \tag{2.14}$$

The prediction (2.13) agrees very well with (2.14).

Conductive textile is widely used as a new

kind of intelligent material[25], the classic Ohm law is not valid for calculation of the resistance for intelligent textile.

The Ohm's resistance formulation for metals reads

$$R \sim \frac{L}{A}, \tag{2.15}$$

where R is the resistance, L length of the metal wire, A its section area.

This scaling (2.15) is valid only for the case of plentiful free electrons in the conductor. For non-metal material, (2.15) should be modified as

$$R \sim \frac{L}{A^{D/(D+1)}}. \tag{2.16}$$

Here D=2 for case when moving charges are distributed on a section, and D=1 if the moving charges are distributed only on its surface(see Fig.3a).

For conductive textile we have

$$R \sim \frac{L}{A^{2/3}}. \tag{2.17}$$

If we want to design an electrochemical cell constructed of two electrodes, which are made of knitted, woven or non-woven conductive textile material, the allometry leads to the following formulation

$$R = k\frac{L}{cA^{2/3}}, \tag{2.18}$$

where k a constant, L the distance between the electrodes, A the surface area of the electrodes, and c the concentration of the electrolyte solution.

The current in electrospinning consists of two parts: the Ohmic bulk conduction current (J_c), and surface convection current(J_s), see Fig.3a and Eq.3.5. The resistance for surface convection scales as

$$R \sim \frac{1}{A^{1/2}}. \tag{2.19}$$

For the surface convection current, we have

$$J_s \sim R^{-1} \sim A^{1/2} \sim r, \tag{2.20}$$

which corresponds to $J_s = 2\pi r\sigma u$ (see Eq.3.5) compared with the Ohmic bulk conduction current $J_c = \pi r^2 kE \sim r^2$.

The scaling(2.17) is also valid for calculation of the resistance for nerve fiber where current is activated due to excitation(see Fig.2). Hodgkin-Huxley equations[26] describe ionic currents of the squid giant axon. The research on Hodgkin – Huxley model is carried out along two directions. One is experiment study, i.e. obtain data with advanced experimental technologies so as to improve the mathematics form of Hodgkin – Huxley model. The other is mathematical analysis on the model. Due to the character of multi-parameters, strong coupling and non-linear, non-linear theories such chaos and bifurcation are widely used to perform the analysis[27]. Despite that these studies show promising indicative results, resistance formulation is still based on Ohm law, which leads to inaccuracy of Hodgkin – Huxley model.

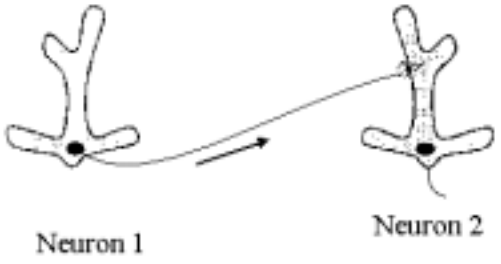

Fig.2 *Resistance in the neural action potential propagation.* $R \sim L/r^{4/3}$, *where r radius of the fiber, L internodal length.*

3. Allometrical Scaling Laws in Electrospinning

Understanding the regulation of allometry in electrospinning would have broad implications on furthering our knowledge of the process and on controlling the diameter of the electrospun fibers. Several authors have described experiments and searched for a ubiquitous

scaling law in electrospinning, the most used scale was $r \sim z^{-1/4}$, but have not given theoretical discussions of their mechanics in different stages in the procedure of electrospinning.

Spivak *et al.* obtained the following relation[8]:

$$\frac{d}{dZ}\left[R^{-4}+(N_w R)^{-1}-N_E^{-1}R^2-N_R^{-1}(\frac{dR^{-2}}{dZ})^m\right]=1, \tag{3.1}$$

where R is the dimensionless jet radius, Z is the dimensionless axial coordinate, N_w, N_E and N_R are, respectively, the Weber number, Euler number, and the effective Reynolds number. Spivak *et al.*[9] obtained a power-law asymptote with an exponent –1/4 for the jet radius:

$$R \sim Z^{-1/4} \quad . \tag{3.2}$$

Shin *et al.*[7] reported an experimental investigation of the electrically forced jet, and the data reveals that the radius decreases as z increases. Fridrikh *et al.*[3] gave a simple analytical model for the forces that determine jet diameter during electrospinning as a function of surface tension, flow rate, and electric current in the jet.

Rutledge's group suggest the following scaling law

$$r \sim z^{-1} \quad (r=\frac{\sqrt{6\mu\rho Q^2}}{\pi IE}\frac{1}{z}), \tag{3.3}$$

in their project No. M01-MD22 "electrostatic spinning and properties of ultrafine fibers", National Textile Center.

Ganan-Calvo and his group[4,5,6] suggested some asymptotic scaling laws in electrospraying. This paper predicts the radius of the jet by allometric scaling.

In this paper, we consider a steady state flow of an infinite viscous jet pulled from a capillary orifice and accelerated by a constant external electric field.

Conservation of mass gives

$$\pi r^2 u = Q, \tag{3.4}$$

where Q is the volume flow rate, r is radius of the jet, u is the velocity.

Letting the surface density of charge be σ, conservation of charges gives[2,7]

$$2\pi r u\sigma + k\pi r^2 E = I, \tag{3.5}$$

where k is the dimensionless conductivity of the fluid, E applied electric field, and I is the current passing through the jet.

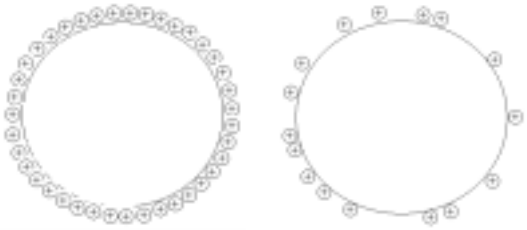

(a) (b)

Fig.3 *Surface charge distribution: (a) full surface charge, (b) partly surface charge*

For the case of partly charged jet in electrospinning (see Fig.3b), Eq.(3.5) can be modified as

$$2\pi r u\sigma^{\alpha} + k\pi r^2 E = I, \tag{3.5a}$$

where α is a surface charge parameter, when $\alpha = 0$ no charge in jet surface, and in case $\alpha = 1$(see Fig.3a), Eq.(3.5a) becomes (3.5). The value of α depends upon dielectric character and/or the salt concentration added in the solution, when $\alpha \neq 1$, the value of α can be considered fractal dimension of charge distribution on a section.

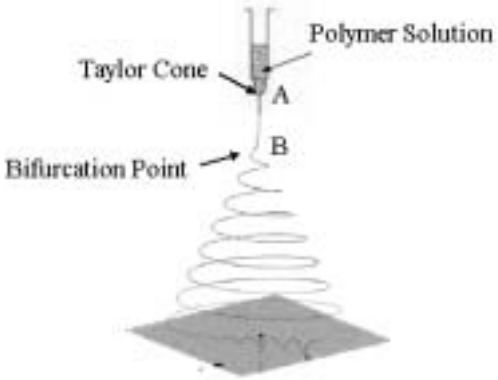

Fig.4 *Bifurcation-like instability in electrospinning.*

Force balance gives[2,7]

$$\rho\frac{d}{dz}(\frac{u^2}{2})=-\frac{\partial p}{\partial z}+\frac{2\sigma E}{r}+\frac{d\tau}{dz}+\rho g\ , \qquad (3.6)$$

where p is the internal pressure of the fluid, g body force, ρ is the liquid density, τ is viscous force.

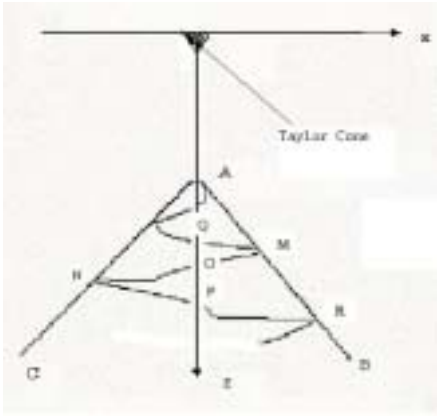

Fig.5 *Instability mechanism of electrospinng*

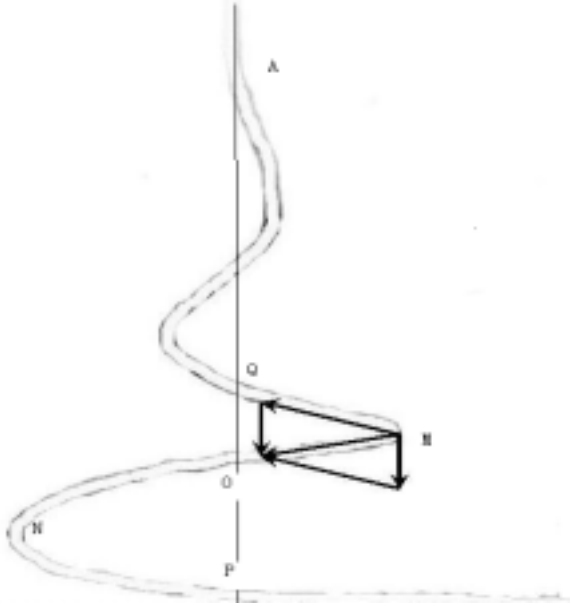

Fig.6 *Instability analysis*

In the absence of an electric field, a meniscus is formed at the exit of the capillary. The meniscus is pulled out into a cone(called Taylor cone, see Fig.4 or Fig.5) when the electric force is applied. It was shown that a conducting fluid can exist in equilibrium in the form of a cone under the action of an electric field but only when the semivertical angle is 49.3^o[28]. When the electric force surpasses a threshold value, the electric force exceeds the surface tension, and a fine charged jet is pulled out and is accelerated. Under the condition of high voltage, calculations and experiment indicated that spinning velocity probably reached and perhaps exceeds the velocity of sound in air.

Fig.7 *A simple pendulum, an analogy to the instability in electrospinning*

When the jet is accelerated by the electrical force, the viscous resistance, $\pi r^2 d\tau/dz$, becomes higher and higher, and the jet becomes instability when the value of the viscous resistance almost reaches or surpasses that of the electrical force, $2\pi r\sigma E$. Under such a condition, a slight perturbation by air might lead to oscillation, see Fig.6. When the moving fiber moves to the boundary AB(conical envelope), for example at M, the velocity in *x*-direction becomes zero, there are three main forces acting on the fiber, viscous force, electronic force, and inertia force. The direction of viscous force is in the inverse direction of its motion, i.e., in the direction of MQ (See Fig.6), the direction of the combining force of electronic force and inertia force is in z-direction, by the parallelogram law, it moves in the direction of its diagonal, i.e. the direction of MO. At the point M, it has the maximal acceleration, and when it reaches the point O, the velocity in x-direction becomes maximum while its acceleration becomes zero, due to inertia, it moves to another boundary AC(see Fig.5). The instability motion in

electrospinning is analogy to pendulum motion as illustrated in Fig.7

When $z \to \infty$ (i.e., close to the jet breakup), surface charge advection is dominant, and the velocity in z-direction keeps unchanged.

The process just likes parachute jump. Initially it accelerates due to the gravity of parachuter, and its velocity becomes higher and higher; while the velocity increases, the air resistance increases while its acceleration decelerates until it become zero.

Many experiment shows scaling relationship between r and z , which can be expressed as an allometric equation of the form

$$r \sim z^b, \tag{3.7}$$

where b is the power exponent.

Assume that the volume flow rate(Q) and the current (I) keep unchanged during the electrospinning procedure, we have the following scaling relations: $Q \sim r^0$, and $I \sim r^0$.

From Eq.(3.4) and Eq.(3.5), we have

$$u \sim r^{-2}, \tag{3.8}$$

$$\sigma \sim r, \tag{3.9}$$

and

$$E \sim r^{-2}. \tag{3.10}$$

3.1 Initial stage for steady streams

At the initial stage of the electrospinning, electrical force is dominant over other forces acting on the jet(i.e., the jet *AB* in Fig.5). Under such a case, Eq.(3.6) can be approximately expressed as

$$\frac{d}{dz}\left(\frac{u^2}{2}\right) = \frac{2\sigma E}{\rho r}. \tag{3.11}$$

Substituting (3.8), (3.9), and (3.10) into (3.11), we have

$$\frac{d}{dz}(r^{-4}) \sim r^{-2}, \tag{3.12}$$

which leads to the following scaling:

$$r \sim z^{-1/2}. \tag{3.13}$$

The scaling relation (3.13) is different from that suggested by Spivak *et al*. [9]. Our prediction (3.13) is valid only for the case when the electrical force acting on the jet dominates over body force, viscous force, and the internal pressure of the fluid, i.e. *AB* in Fig.5.

In order to verify our prediction, we re-analysis the experimental data in open literature. Fig.8 and Fig.9 show Taylor's[28] and Spivak *et al.*'s original experimental data[9], Fig.10 and Fig.11 illustrate, respectively their scaling relations at initial stages.

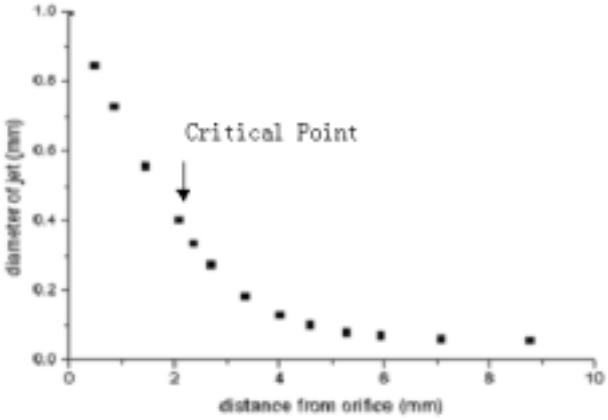

Fig. 8 *Taylor's original experimental data*[28]

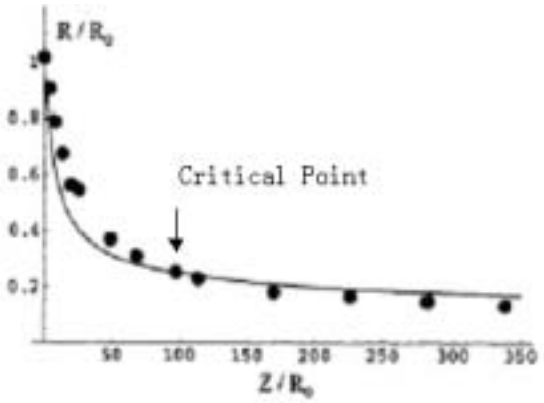

Fig.9 *Spivak et al.'s original experimental data*[9].

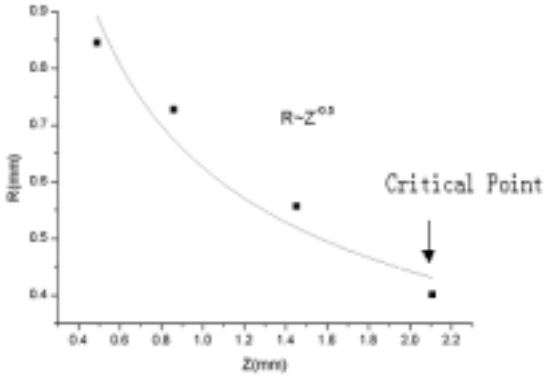

Fig.10 *Comparison of our prediction of* (3.13) (*continued line*) *with Taylor's experimental data*[28].

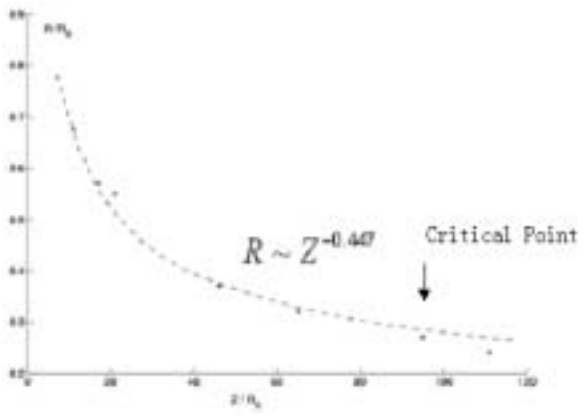

Fig.11 *Comparison of our prediction of* (3.13) (*dashed line*) *with Spivak et al.'s experimental data*[9].

3.2 Instability of viscous jets

Under some circumstances a jet was observed which appeared to rise steadily for a short distance and then to disappear suddenly. Instability occurs when combining force of the electric and viscous forces approximately vanishes, i.e.,

$$\frac{2\sigma E}{r}+\frac{d\tau}{dz}\approx 0\,. \tag{3.14}$$

We assume that the gradient of pressure keeps unchanged during this stage, i.e.,

$$\frac{dp}{dz}=\text{constant}\,. \tag{3.15}$$

The N-S equation (3.6), under the instability condition, reduces to

$$\frac{d}{dz}(\frac{u^2}{2})=-\frac{1}{\rho}\frac{dp}{dz}=\text{constant}\,. \tag{3.16}$$

In view of the scaling relation, (3.8), we have

$$\frac{d}{dz}(r^{-4})\sim r^0, \tag{3.17}$$

from which we obtain the following scaling law

$$r\sim z^{-1/4}\,. \tag{3.18}$$

The result is same as that in open literature, see Fig.12. Now write τ in the form

$$\tau=\mu\frac{du}{dz}\,. \tag{3.19}$$

Write (3.14) in a scaling form

$$\frac{2\sigma E}{r}+\mu\frac{d^2u}{dz^2}\sim r^0\,. \tag{3.20}$$

Substituting (3.8), (3.9), and (3.10) into (3.20), we immediately obtain the following scaling law between the radius of fiber and the viscosity:

$$r\sim\mu^{1/2}\,, \tag{3.21}$$

Our prediction (3.21) satisfies exactly the experimental data obtained by Baumgarten[29].

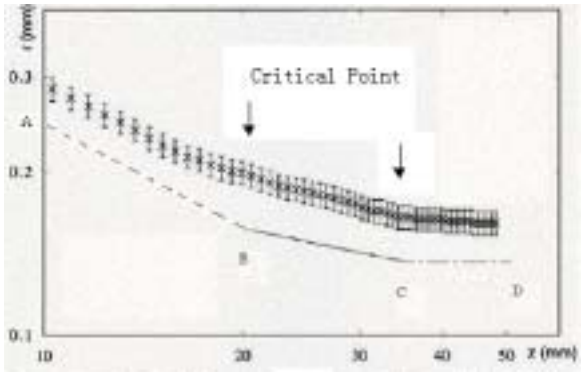

Fig.12 *Shin et al.'s experimental data. The dashed line (AB) corresponds to the slope of a line that scales as* $r\sim z^{-0.53}$*; while the solid line* $r\sim z^{-0.25}$*;* $r\sim z^0$ *for CD.*

3.3 Terminal state

When $z\to\infty$, acceleration in z-direction vanishes completely, i.e.,

$$\frac{d}{dz}(\frac{u^2}{2})=0\,, \tag{3.22}$$

which leads to the scaling law

$$r\sim z^0\,. \tag{3.23}$$

4. Conclusion

Our theory predicts $r \sim z^{-0.5}$ in the initial stage (AB in Figs.5,6) when electrically generated force is dominant, $r \sim z^{-1/2}$ for the instability stage, and $r \sim z^{0}$ for the case when $z \to \infty$. Our predictions agree well with the experimental data obtained by Shin *et al.* (See Fig.10) , from Fig.8 we know that *z*=20 is a bifurcation point.

It should be specially pointed out that the scaling relation $r \sim z^{-1/2}$ for the instability stage is only valid for the case 1) resultant force of the electric and viscous forces approximately vanishes, and 2) acceleration become approximately zero.

Acknowledgement

The work is supported by grant 10372021 from National Natural Science Foundation of China. The original idea was suggested by Ji-Huan He, Y.-Q. Wan is a Ph.D. candidate under the supervision of J.-Y. Yu and J.-H. He.

References

[1] Z.-M. Huang, Y.-Z. Zhang, M. Kotaki, S. Ramakrishna, A review on polymer nanofibers by electrospinning and their applications in nanocomposites, *Composites Science and Technology* **63** (2003): 2223–2253

[2] Wan,Y.Q., Guo,Q., Pan,N., Thermo-electro-hydrodynamic model for electrospinning process, *International Journal of Nonlinear Sciences and Numerical Simulation*, **5** (2004):5-8

[3] Fridrikh,S.V., Yu, J.H., Brenner, M.P., and Rutledge G.C., Controlling the Fiber Diameter during Electrospinning, *Phys. Rev. Lett.* **90**(2003): 144502

[4] Ganan-Calvo,A.M., Cone-jet analytical extension of Taylor's electrostatic solution and the asymptotic universal scaling laws in electrospraying, *Phy. Rev. Lett.*, **79**(2), 1997: 217-220.

[5] Ganan-Calvo,A.M., The surface charge in electrospraying: its nature and its universal scaling laws, *J. Aerosol Sci.*, **30**(7),1999: 863-872

[6] Ganan-Calvo,A.M., Davila,J., Barrero,A. Current and droplet size in the electrospraying of liquids. Scaling laws, *J. Aerosol Sci.*, **28**(2),1997: 249-275

[7] Shin,Y.M, Hohman,M.M., Brenner,M.P., Rutledge,G.C., Experimental characterization of electrospinning: the electrically forced jet and instabilities, *Polymer*, **42**(2001): 9955-9967

[8] Spivak, A.F. and Dzenis, Y.A. Asymptotic decay of radius of a weakly conductive viscous jet in an external electric field, *Applied Physics Letters*, **73**(21), 1998: 3067-3069

[9] Spivak, A.F., Dzenis, Y.A., and Reneker,D.H. A model of steady state jet in the electrospinning process, *Mechanics Research Communications*, **27**(1), 2000: 37-42

[10] West, B.J. Comments on the renormalization group, scaling and measures of complexity, Chaos, Solitons and Fractals, **20**(2004): 33-44

[11] Harris G.H. *Introduction to modern theoretical physics*, John Wiley & Sons, 1975

[12] Iovane, G. Varying *G*, accelerating universe, and other relevant consequences of a stochastic self-similar and fractal universe, *Chaos, Solitons and Fractals*, **20**, 2004, 657-667

[13] He JH, Chen, H. Effects of Size and pH on Metabolic Rate, *International Journal of Nonlinear Sciences and Numerical Simulation*, **4** (2003): 429-432

[14] Kuikka JT. Scaling Laws in Physiology: Relationships between Size, Function, Metabolism and Life Expectancy, *International Journal of Nonlinear Sciences and Numerical Simulation*, **4** (2003): 317-328

[15] Kuikka JT. Fractal analysis of medical imaging, *International Journal of Nonlinear Sciences and Numerical Simulation*, **3** (2002): 81-88

[16] West GB, Brown JH, Enquist BJ. A general

model for origin of allometric scaling laws in biology, *Science*, **276**(5309), 1997: 122-126

[17] Huxley JS problems of relative growth, New York: the Dial Press, 1932

[18] Taylor LR Aggregation, variance and the mean, Nature, 1961, 189: 732

[19] Pareto V. Manuale di exonomia politica, Milano, Societa Editrice, 1906, Cours d'Economie Politique, Lausanne and Paris, 1879

[20] Benzi R. Getting a grip on turbulence, *Science*,**301**(5633), 2003,605-606

[21] Chen H, Kandasamy S, Orszag S, Shock R, Succi S, and Yakhot V. Extended Boltzmann kinetic equation for turbulent flows, *Science*, **301**(5633),2003,633-636

[22] Banavar,JR., Maritan,A., Rinaldo,A. Nature, 399, 1999, 130-132

[23] Dreyer,O., Puzio,R., Allometric scaling in animals and plants, *J. Math. Biol.*, 43, 2001, 144-156

[24] Tacx, J.C.J.F., Schoffeleers, H.M., Brands, A.G.M., Teuwen, L. *Polymer* **41** (2000) 947.

[25] Nouri,M., Kish,M.H., Entezami,A.A., Edrisi,M., Conductivity of textile fibers treated with aniline, *Iranian Polymer Journal*, **9**(1),2000: 49-58

[26] Hodgkin, A.L., Huxley, A.F., A quantitative description of membrane current and its application to conduction and excitation in nerve. J. Physiol. *117*, 1952: 500-544.

[27] Jiang,W., Tsang, K. M., Hua, Z. Hopf bifurcation in the Hodgkin–Huxley model exposed to ELF electrical field, *Chaos, Solitons and Fractals*, **20** (2004) 759–764

[28] S. G. Taylor, Electrically driven jets (with an appendix by M.D. Van Dyke), Proc Roy Soc London A. **313**(1969):453-475

[29] P.K. Baumgarten, Electrostatic spinning of acrylic microfibers, *J. Colloid Interface Sci.* **36**(1),1971: 71-79